

Sarah Duenwald-Kuehl

Department of Biomedical Engineering,
University of Wisconsin,
Madison, WI 53706

Hirohito Kobayashi

Department of Orthopedics,
University of Wisconsin,
Madison, WI 53706

Roderic Lakes

Departments of Biomedical Engineering
and Engineering Physics,
University of Wisconsin,
Madison, WI 53706

Ray Vanderby, Jr.¹

Departments of Biomedical
Engineering and Orthopedics,
University of Wisconsin,
Madison, WI 53706
e-mail: vanderby@ortho.wisc.edu

Time-Dependent Ultrasound Echo Changes Occur in Tendon During Viscoelastic Testing

The viscoelastic behavior of tendons has been extensively studied in vitro. A noninvasive method by which to acquire mechanical data would be highly beneficial, as it could lead to the collection of viscoelastic data in vivo. Our lab has previously presented acoustoelasticity as an alternative ultrasonic-based method of measuring tendon stress and strain by reporting a relationship between ultrasonic echo intensity (B mode ultrasound image brightness) and mechanical behavior of tendon under pseudoelastic in vitro conditions [Duenwald, S., Kobayashi, H., Frisch, K., Lakes, R., and Vanderby Jr., R., 2011, "Ultrasound Echo is Related to Stress and Strain in Tendon," J. Biomech., 44(3), pp. 424–429]. Viscoelastic properties of the tendons were not examined in that study, so the presence of time-dependent echo intensity changes has not been verified. In this study, porcine flexor tendons were subjected to relaxation and cyclic testing while ultrasonic echo response was recorded. We report that time- and strain history-dependent mechanical properties during viscoelastic testing are manifested in ultrasonic echo intensity changes. We also report that the patterns of the echo intensity changes do not directly mimic the patterns of viscoelastic load changes, but the intensity changed in a repeatable (and therefore predictable) fashion. Although mechanisms need further elucidation, viscoelastic behavior can be anticipated from echo intensity changes. This phenomenon could potentially lead to a more extensive characterization of in vivo tissue behavior. [DOI: 10.1115/1.4007745]

Keywords: tendon, ultrasound, echo intensity, acoustoelasticity

1 Introduction

Tendons connect muscle to bone, facilitating joint movement and stabilization. Tendons also store and release energy during motion [1]. The mechanical properties of the tendon are therefore critical to tendon function and understanding the viscoelastic, or time- and history-dependent, behavior of tendons is essential. Customary methods of viscoelastic testing involve the use of animal models [2–5] or cadaveric tissues [6,7] and extraction from the body for testing in a mechanical test system, precluding direct study of viscoelasticity in healthy, live tendons in their natural configuration. The first step in such *in vivo* testing is a method by which time-dependent information can be gathered noninvasively.

Because of its speed, safety, and affordability, ultrasound-based techniques are gaining popularity for the evaluation of tissue properties. Speckle tracking can be used to measure displacement and strain in the tissue [8,9]. Using traditional elastography, tracked tissue displacement can be used to infer tissue stiffness [10,11]; this information can then be used to detect changes in tissue properties (i.e., stiffening of tumors) for diagnosis purposes [12]. Wave propagation velocity through the tissue (i.e., speed of sound) can also be measured [13]. Using shear wave sonoelastography, propagation of shear waves through the tissue of interest can be measured and used to estimate tissue elasticity [14,15], which can also be used to distinguish between tissue types (i.e., benign versus malignant tumors) [16,17]. Acoustoelastic theory, originally developed by Hughes and Kelly [18], relates changes in mechanical properties stress, strain, and stiffness to acoustic wave velocity and amplitude [19]. Acoustoelastography, one applica-

tion of acoustoelastic theory, is based on the relationship between ultrasonic wave amplitude and mechanical stiffness and strain. In one study, Kobayashi and Vanderby derived a relationship between reflected A-mode ultrasonic wave amplitude and mechanical behavior in pseudoelastic, incompressible materials [20]; applied strains and normalized material coefficients (i.e., normalized stiffness) were determined from reflected ultrasound wave data acquired while stretching rubber. As the rubber was deformed, the stiffness increased and the magnitude of the reflected ultrasound increased in a predictable manner.

This increased amplitude of the reflected ultrasound wave indicates that the brightness of clinical B-mode images, or the “echo intensity,” should increase with applied strain. This phenomenon was verified in an *in vitro* B-mode ultrasound study, as tensioning tendons increased the intensity of reflected ultrasound echo, leading to a brighter image [21]. A second *in vitro* study by Pan et al. demonstrated a similar increase in echo intensity with increased strain level in skin [22]. The presence of time-dependent echo intensity changes as a result of viscoelastic behavior during *in vitro* testing, however, has not been verified. The presence of such changes would have implications in any ultrasound-based mechanical estimation, and would have to be considered when designing experimental protocols. The purpose of this study, therefore, is to test the hypothesis that viscoelastic tendon behavior affects ultrasonic echo intensity from B-mode images in a reproducible and consistent fashion. If experiments support this hypothesis, clinical ultrasound systems would hold the potential to noninvasively quantify viscoelastic behavior.

2 Materials and Methods

2.1 Specimen Preparation. Porcine flexor tendons ($n = 15$) were excised from 15 limbs obtained from a local abattoir, with care to keep the bony insertion intact while removing all

¹Corresponding author.

Contributed by the Bioengineering Division of ASME for publication in the JOURNAL OF BIOMECHANICAL ENGINEERING. Manuscript received April 24, 2012; final manuscript received August 1, 2012; accepted manuscript posted September 29, 2012; published online October 26, 2012. Editor: Victor H. Barocas.

extraneous tissue. The distal bone was potted in lightweight filler (Evercoat, Cincinnati, Ohio) molded to match the interior of the lower grip for a more secure hold. The proximal end of the tendon was cleaned of all muscle tissue and the cross-sectional area (assumed elliptical) was measured using calipers at three points along the length of the tendon and averaged. Specimens were then loaded into the mechanical test system (MTS Bionix, Minneapolis, MN) equipped with a bath filled with physiologic buffered saline (which served to both keep the tendon hydrated and transmit ultrasound waves), a 1000 lb load cell (Honeywell, Morristown, NJ), and custom-made grips [23], preloaded to 1 N, and preconditioned for 20 s at 0.5 Hz using a sinusoidal wave to 2% strain (using grip-to-grip displacement and initial length measurements), followed by a 1000 s rest period.

2.2 Mechanical Testing. Tendons were split into two testing groups. Group 1 ($n = 10$) tendons were subjected to (1) stress relaxation at 4% strain (40 ms rise time, considered a step displacement, held for 100 s), followed immediately by a partial recovery at 2% strain (100 s), as well as to (2) cyclic testing between 0% and 4% strain (10 cycles at 0.5 Hz). Each specimen underwent three of each type of test (in randomized order) for a total of six tests. A rest period of 1000 s (at zero strain) was allowed between each test.

Group 2 ($n = 5$) tendons were subjected to stress relaxation testing at 1%, 2%, 3%, 4%, 5%, and 6% strain (100 s). Each specimen underwent one test at each strain level in randomized order, with a rest period of 1000 s between each test.

2.3 Ultrasound Analysis. B-mode cine ultrasound was recorded (20 frames/s) during mechanical testing using a GE 12L-RS Linear Array Transducer at 12 MHz and GE LOGIQe ultrasound (General Electric, Fairfield, Connecticut). The ultrasound transducer was clamped in a fixed position (the bottom of the transducer lined up with the bottom grip, 4 cm from the front surface of the tendon, focused on the midline of the tendon) in a custom platform connected to the testing bath (see Fig. 1).

The overall echo intensity (defined as the average gray scale brightness of the selected region in the B-mode image) of the tendon, averaged over the entire region of interest (ROI), which consisted of the entire visible area between the grips (front to back surface along the midline), was calculated for each frame in order to record the echo intensity changes over time (EchoSoft, Echometrics, Madison, Wisconsin). Previous studies have shown that porcine flexor tendon relaxation and recovery follow a power

law behavior in time, with the largest stress changes occurring in the first few seconds [23,24]. Thus, echo intensity was recorded during the first 5 s of relaxation testing and during the first 5 s of recovery from relaxation. Likewise, the flexor tendons exhibit transient behavior during early cycles of cyclic testing at 0.5 Hz but behave in pseudoelastic fashion by cycle 8; thus, echo intensity was recorded during the first three cycles (a total of 6 s) of the cyclic testing.

2.4 Parameter Calculation. Force data from the MTS were used to calculate stress (1st Piola Kirchoff). Data collected during the stress relaxation testing of group 1 specimens were used to calculate the maximum echo intensity change (represented as percent change from the resting echo intensity, see Fig. 2(a)) as well as the echo intensity change during the 5 s of relaxation (the difference between the echo intensity values at the onset of relaxation and the echo intensity values after 5 s of relaxation, see Fig. 2(a)). Corresponding mechanical parameters maximum stress (see Fig. 2(c)) and stress decrease during the first 5 s of relaxation (Fig. 2(c)) were calculated from mechanical data (stress is calculated by dividing force by initial area). Data collected from the recovery portions of the testing was also analyzed to calculate the decrease in echo intensity during the first 5 s of recovery (see Fig. 2(b)). The stress increase occurring during the first 5 s of recovery from relaxation was also calculated (Fig. 2(d)). See Table 1 for full parameter definitions.

Data collected during the cyclic testing of group 1 specimens were used to calculate the peak echo intensity change (represented as percent change from the resting echo intensity, Fig. 3(a)) as well as the echo intensity difference between the first and third cycle (the difference between the peak echo intensity of the first curve and the peak echo intensity of the third curve, Fig. 3(a)). Likewise, the peak stress reached during cyclic testing (Fig. 3(b)) and the decrease in peak stress between the first and third cycle (Fig. 3(b)) were calculated.

Data collected during the stress relaxation testing of group 2 specimens were used to calculate the maximum echo intensity change (represented as percent change from the resting echo intensity, see Fig. 2(a)) and maximum stress (see Fig. 2(c)) reached during the 5 s of relaxation at each strain level.

An ANOVA was performed on the mechanical and ultrasound results at various strains to determine statistical significance between maximum values at each strain level. Statistically significant differences were assumed for $p \leq 0.05$.

3 Results

The average parameter value from the three trials was used for analysis. Separate trials on each specimen gave repeatable echo intensity changes, with deviation of less than 10% of the mean for all parameters (deviations were 4.48%, 8.30%, 2.96%, 3.79%, and 6.12% of the mean for peak echo intensity change during cyclic testing, increase in peak intensity between first and third cycles, maximum echo intensity during relaxation, increase in echo intensity during relaxation, and decrease in echo intensity during recovery from relaxation, respectively).

Stress during relaxation followed a power law behavior in time, and echo intensity increased with time. The maximum echo intensity change reached during relaxation testing at 4% strain was $10.45 \pm 0.94\%$ (mean \pm standard deviation), while the echo intensity change during the 5 s of relaxation was $3.12 \pm 0.35\%$ (Fig. 4(a)). The echo intensity decrease in the first 5 s of recovery following relaxation was $5.51 \pm 1.11\%$ (Fig. 4(b)). The corresponding maximum stress reached during relaxation testing at 4% strain was 3.07 ± 1.25 MPa, with a 0.64 ± 0.19 MPa decrease in stress over the first 5 s of relaxation (Fig. 4(c)). The stress increase during the first 5 s of recovery following relaxation was 0.032 ± 0.009 MPa (Fig. 4(d)). Echo intensity changes are negatively correlated with stress changes during (Fig. 4(e)) relaxation ($R^2 = 0.79435$) and (Fig. 4(f)) recovery ($R^2 = 0.90622$).

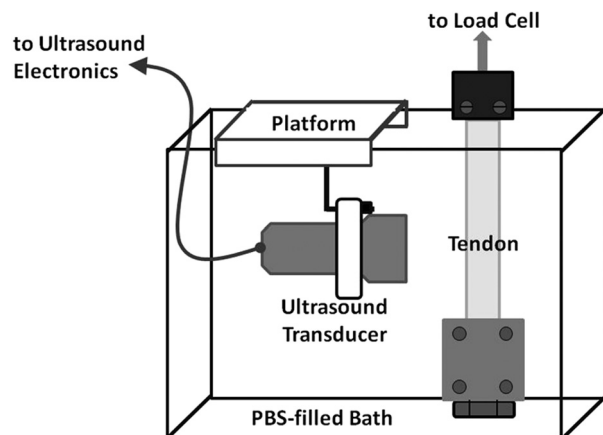


Fig. 1 Ultrasound bath setup used for mechanical and ultrasound testing; tendons were gripped in a stainless steel bone block (stationary) and a custom soft tissue grip (attached to actuator), the ultrasound transducer was fixed to a platform for repeatable positioning. The bath was filled with saline to maintain tissue hydration and facilitate ultrasound wave propagation.

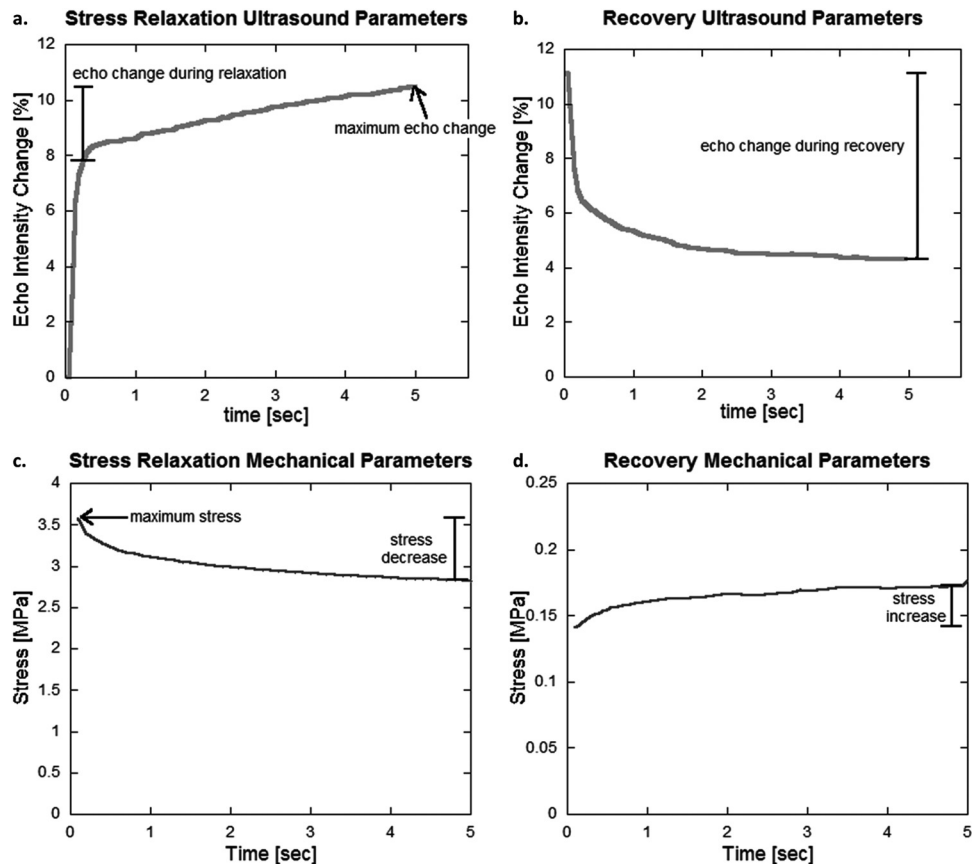


Fig. 2 Ultrasound parameters collected during (a) stress relaxation and (b) recovery testing, and mechanical parameters collected during (c) stress relaxation and (d) recovery testing. Ultrasound parameters include maximum echo intensity change (comparable to max stress in (c)), echo change during relaxation (comparable to stress decrease in (c)), and echo change during recovery [comparable to stress increase in (d)]. Note that the initial jumps in echo intensity and stress correspond to the jump in load that accompanies the step displacement input.

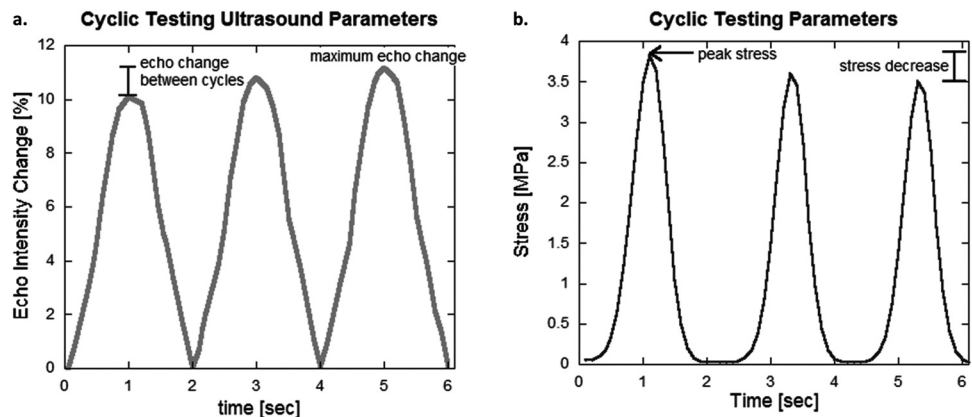


Fig. 3 Cyclic testing parameters for (a) ultrasound testing and (b) mechanical testing, including maximum echo intensity change (comparable to peak stress) and echo change between cycles (comparable to stress decrease)

Peak echo intensity change reached during cyclic testing at 4% strain was $10.71\% \pm 1.42\%$, and the increase in peak echo intensity between the first and third cycles was $1.42 \pm 0.60\%$ (Fig. 5(a)). The peak stress reached during cyclic testing at 4% strain was 3.25 ± 1.33 MPa, and the decrease in peak intensity from the first and third cycles was 0.21 ± 0.08 MPa (Fig. 5(b)). Echo intensity changes are negatively correlated with stress changes (Fig. 5(c)) during cyclic testing ($R^2 = 0.82809$).

Echo intensity change increased as the relaxation strain increased (Fig. 6(a)). Maximum echo intensity changes during relaxation at 1%, 2%, 3%, 4%, 5%, and 6% strain were $2.40 \pm 0.67\%$, $6.02 \pm 0.40\%$, $8.34 \pm 0.82\%$, $10.58 \pm 0.58\%$, $12.70 \pm 1.08\%$, and $16.29 \pm 1.55\%$, respectively. Likewise, stress increased as the relaxation strain increased (Fig. 6(b)). Maximum stress during relaxation at 1%, 2%, 3%, 4%, 5%, and 6% strain were 0.25 ± 0.05 MPa, 0.71 ± 0.13 MPa, 1.64 ± 0.29 MPa,

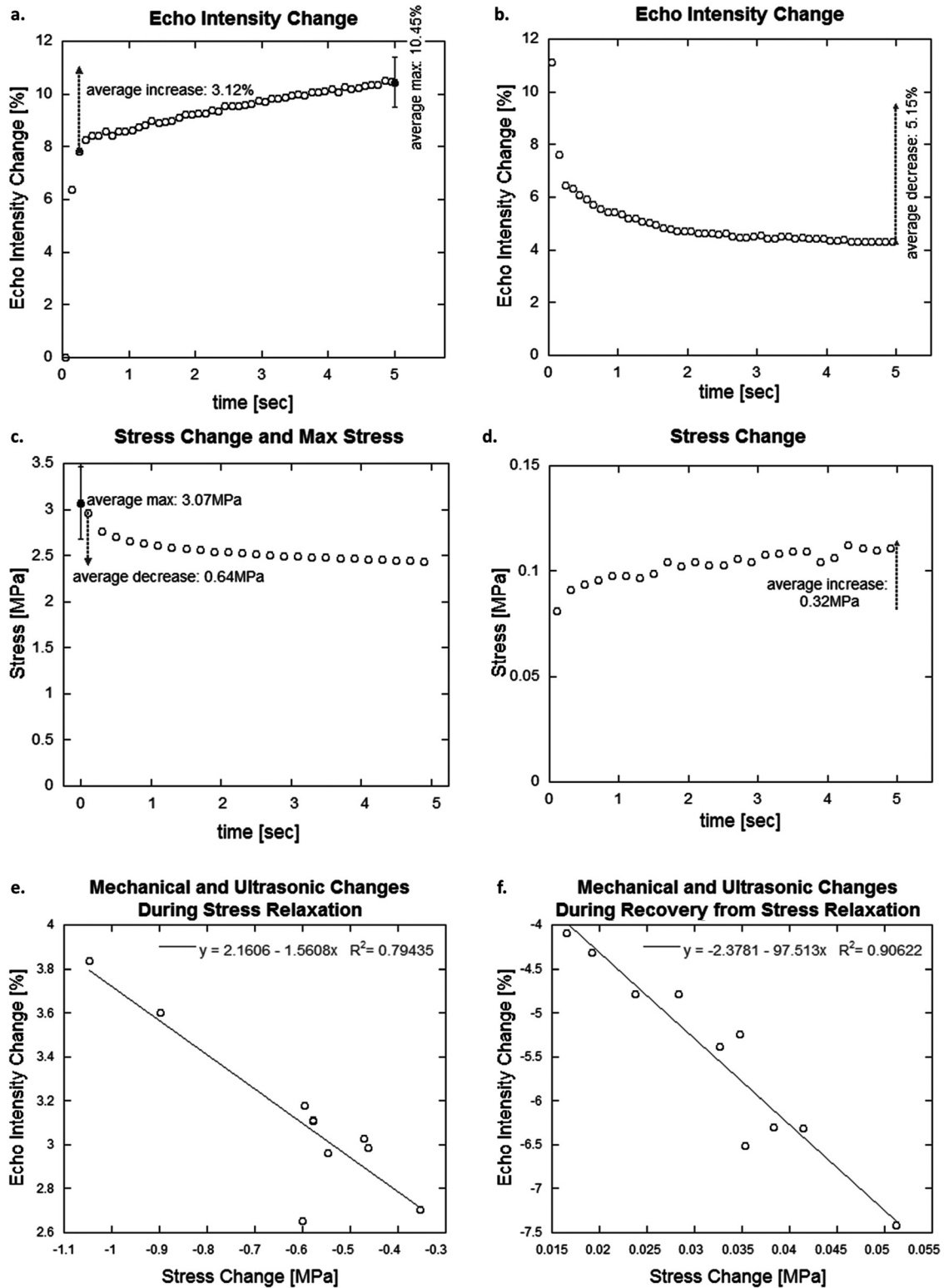


Fig. 4 Echo intensity and stress changes during stress relaxation and recovery from relaxation. (a) Echo intensity increases during stress relaxation at 4% strain; (b) echo intensity decreases during recovery (at 2% strain) from relaxation. (c) Maximum stress reached and stress decreases during relaxation at 4% strain; (d) stress increases during recovery (at 2% strain) from relaxation. Results demonstrate the stress or echo intensity changes of one representative specimen (open circles indicate data points) together with the average results of all 10 specimens, including average increase/decrease (dotted arrow) and average maximum echo intensity (filled circle with error bars). Error bars indicate one standard deviation. Note that the echo intensity response includes a sharp increase/decrease during step displacement as well as steady increase/decrease during relaxation/recovery. Also note that the echo intensity during recovery does not return fully to zero in the 5 s plotted, which would be anticipated based on the slower rate of recovery [23]. Echo intensity changes are negatively correlated with stress changes during (e) relaxation ($R^2 = 0.79435$) and (f) recovery ($R^2 = 0.90622$).

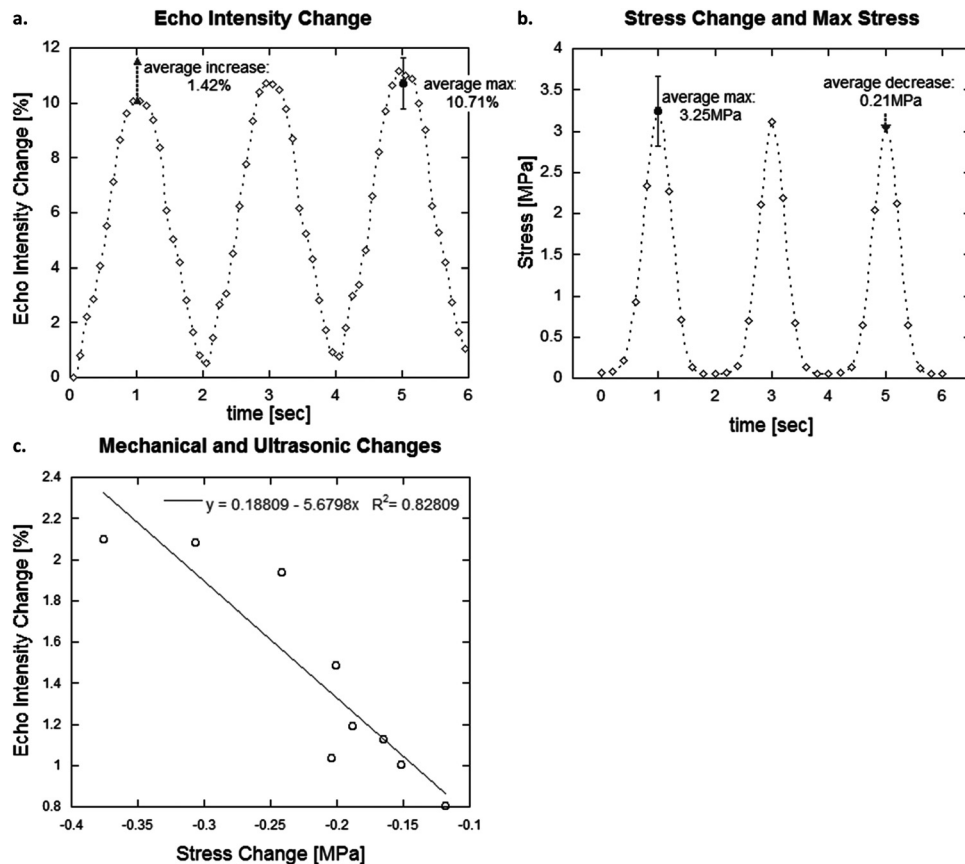


Fig. 5 (a) Echo intensity changes and (b) mechanical stress changes during cyclic testing to 4% strain. Results demonstrate the echo intensity and stress changes of one representative specimen (open symbols represent data points) together with the average results of all specimens in the group, including average maximum echo intensity change and maximum stress (filled symbols with error bars) and average increase/decrease (dotted arrow). Error bars indicate one standard deviation. (c) Echo intensity changes are negatively correlated with stress changes during cyclic testing ($R^2 = 0.82809$).

3.11 ± 0.43 MPa, 5.06 ± 0.74 MPa, and 8.14 ± 0.84 MPa, respectively. Maximum echo intensity and stress were significantly different at each strain level ($p < 0.001$ for each case), and a logarithmic relationship exists between maximum echo intensity change and strain level (Fig. 6(c); $R^2 = 0.8983$).

4 Discussion

We have previously reported the correlation between ultrasound echo intensity changes and stress and strain in the tendon under pseudoelastic conditions. In this study we examined the presence of nonelastic echo intensity changes in response to viscoelastic testing. In particular, stress relaxation, recovery from relaxation, and the initial three cycles of cyclic testing were examined. In each case, time- and strain history-dependent echo intensity changes were observed. This study therefore supports our hypothesis that time-dependent tendon behavior affects ultrasonic echo intensity from B-mode images in a reproducible and consistent fashion.

During the step strain input of stress relaxation testing, echo intensity increased sharply (Fig. 4(a)). This sharp increase in echo intensity mimics the sharp increase in both load and strain during the step displacement. As the strain was held during further relaxation, the echo intensity continued to increase at a steady rate. The continued increase in echo intensity differs in behavior from both load (which decreases at a steady rate during relaxation) and strain (which is held constant).

The echo intensity changes observed during stress relaxation increased as the strain input increased. This was evident in both the increase in maximum echo intensity changes and the increased slope of the echo intensity curves as seen in Fig. 6(a).

During recovery from stress relaxation, the trends in echo intensity reversed; echo intensity decreased sharply during the step displacement input (in the negative direction), then continued to decrease at a steady rate during recovery. Similar to the echo intensity changes during relaxation, the sharp decrease in intensity mimics the sharp decrease in both load and strain during the step displacement in the negative direction, but the continued echo intensity decrease differs in behavior from load (which increases during recovery) and strain (which is held constant). The total change in echo intensity during the first 5 s of recovery is less than the total change in echo intensity during the first 5 s of relaxation, which mirrors the rate difference seen between relaxation and recovery (recovery progressing at a slower rate than stress relaxation) in the mechanical results here and in previous mechanical testing [24].

The general shape of the echo intensity changes during cyclic testing was similar to those seen in the pseudoelastic experiments [21], with the exception of the increase in peak echo intensity over the first three cycles. The cyclic changes in intensity mimic the cyclic pattern in displacement and load, but the increase in peak intensity with each cycle differs from load, which has decreasing peak load with each cycle, and displacement, which has the same peak strain with each cycle (Fig. 5).

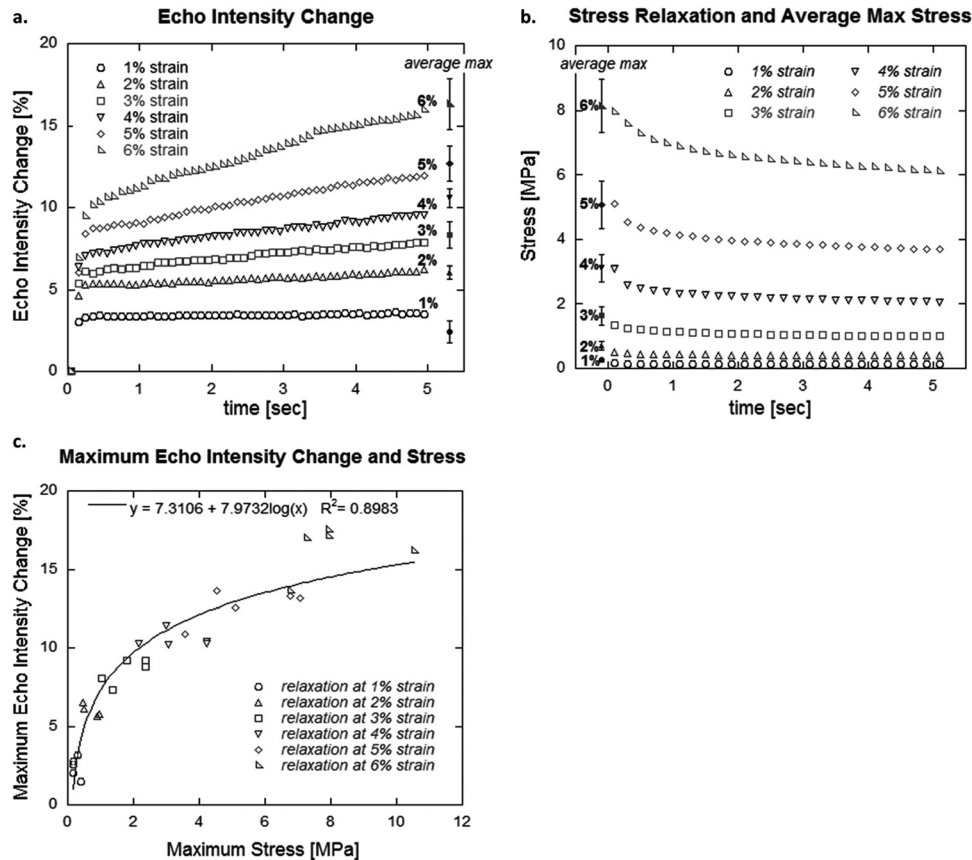


Fig. 6 (a) Echo intensity changes and (b) mechanical stress changes during stress relaxation at various strains. Results demonstrate the echo intensity and stress changes of one representative specimen (open symbols represent data points) undergoing relaxation at 1%, 2%, 3%, 4%, 5%, and 6% strain together with the average results of all specimens in the group for maximum echo intensity change and maximum stress (filled symbols with error bars) at each of the strain levels. Error bars indicate one standard deviation. (c) A logarithmic relationship exists between maximum echo intensity change and strain level ($R^2 = 0.8983$).

Table 1 Parameter definitions

Parameter	Calculation
<i>Relaxation</i>	
Ultrasound Parameters	
max echo intensity change during relaxation	(maximum intensity – resting intensity)/resting intensity \times 100
echo change during first 5 s	% echo intensity change at 5.1 s – % echo intensity change at 0.1 s ^a
Mechanical Parameters	
maximum stress during relaxation	maximum stress (stress at 0.1 s)
stress change during first 5 s	stress at 0.1 s ^a – stress at 5.1 s
<i>Recovery</i>	
Ultrasound Parameter	
echo change during first 5 s	% echo intensity change at 0.1 s – % echo intensity change at 5.1 s
Mechanical Parameter	
stress change during first 5 s	stress at 5.1 s – stress at 0.1 s
<i>Cyclic</i>	
Ultrasound Parameter	
peak echo intensity change (%)	(peak intensity – resting intensity)/resting intensity \times 100
echo change between first three cycles	(% echo intensity change at peak of cycle 3) – (% echo intensity change at peak of cycle 1)
Mechanical Parameter	
peak stress	maximum stress (stress at peak of cycle 1)
stress change between first three cycles	stress at peak of cycle 1 – stress at peak of cycle 3

^aData collection begins at 0.1 s; thus 5 s of relaxation occurs between 0.1 and 5.1 s.

The increasing intensity during relaxation (Fig. 4(a)), as well as the increased peak intensity during the first three cycles of cyclic testing (Fig. 4(a)), is interesting and was not expected. Parameters affecting reflected intensity are stiffness, stress, and

density for a homogeneous material. In tendon, stress is reduced during stress relaxation (Fig. 4(c)) and peak stresses during cyclic testing decrease over the first three cycles (Fig. 5(b)). The unexpected time-dependent increases in echo intensity occurring

during stress relaxation can be correlated to tissue-related mechanisms which may contribute to this phenomenon. Possible mechanisms include the temporal microstructural reorganization [25,26] associated with fiber alignment in the tissue. The intensity changes may also be related to the superposition of reflected waves from various reflector fibers whose spacing could be changing (i.e., a microstructural effect different from the homogenized model predictions). Alternatively, water movement out of the tendon [27–29] may increase local density. The influence of superposition of waves could be investigated by varying the frequency (and thus the wavelength) of the ultrasound signal. The presence of other mechanisms can be confirmed by a series of experiments, i.e., hydration assays for water movement and imaging methods such as polarized microscopy or second harmonic imaging to analyze collagen fibers. However, determining the influence of each mechanism is a complex question, and it would be difficult to perform an experiment that isolates one mechanism (i.e., hydration) without altering other factors as well (i.e., fiber spacing).

Current ultrasound-based methods such as traditional elastography (using wave theory) and acoustoelastography (which draws on the concepts of acoustoelastic theory) do not account for time-dependent behavior associated with viscoelasticity during testing, and would require reformulations to do so. Elastography has some inherent limitations that limit its ability to measure viscoelastic behaviors. For example, the wave theory equations utilized in elastography are not strain dependent, and therefore it uses only an initial and end state for analysis. This precludes it from defining the strain-dependent viscoelastic behavior previously demonstrated in tendon [23,24] unless by linear increments. Furthermore, to avoid errors arising from tissue strain dependence, elastography experiments in soft tissues are traditionally limited to very small (<1% strain) strains; when soft tissues were tested under larger deformations and were therefore nonlinear in stiffness, significant errors occurred [30,31]. Limiting experiments to such small strains could make measuring viscoelastic changes difficult in tendon, as viscoelastic changes at such low strains are smaller than at higher physiologic strains, and the viscoelastic portion of the behavior is a small fraction of the total behavior (i.e., less than 1%) [23,24]. Finally, elastography methods track points from the unloaded to loaded state, inferring stiffness from measured strain; strain alone is not sufficient to describe viscoelastic changes, particularly when considering stress relaxation (as strain remains constant during the test). Acoustoelastic theory equations are strain dependent and incorporate changes in reflected echo, making them more flexible for future reformulations to contain time-dependent parameters. However, neither approach currently considers time-dependent ultrasound changes due to viscoelastic behavior. Researchers must take this into account when designing experiments based on these methods (i.e., making sure the tissue is in a pseudoelastic state with sufficient loading cycles prior to data collection) to avoid time-dependent inconsistencies.

The present study investigated isolated tendons in a controlled environment in order to confirm the presence of time-dependent changes in echo intensity during static and cyclic loading. Translating the method to measure such changes *in vivo* will require addressing challenges associated with traditional ultrasound imaging, such as anisotropy and interposing tissue, and additional issues arising from viscoelastic testing, such as controlling strain history and precise loading protocols. Keeping the transducer parallel to the tendon of interest (or the region of interest on the tendon) will reduce effects of anisotropy. Also, many tendons of interest (i.e. Achilles, patellar, and supraspinatus tendons) are fairly superficial, reducing the effects of interposing tissue. Rest protocols prior to and between tests will allow for viscoelastic recovery in the tendon, and activity restrictions help to control strain history. Use of dynamometers allows for controlled loading and/or displacement, and methods involving muscle stimulators can simulate step loading (creep) methods.

The major limitation of this study is its applicability to *in vivo* measurements. Controlled *ex vivo* loading in a test frame creates ideal conditions which cannot be readily replicated *in vivo*. Additionally, only one tendon is considered (porcine digital flexor tendon), and different tendons may exhibit varying behavior based on composition and viscoelastic characteristics. A weight-bearing tendon was chosen to be functionally similar to commonly injured tendons (i.e., Achilles tendon), but differences may still impair translation. Another limitation of this technique is that grayscale images collected from the clinical ultrasound were log-compressed and digitized from RF signals; this type of image processing may increase measurement error and reduce signal-to-noise. However, the average baseline intensity was 62.0 (on a scale of 0 to 255), and the average noise in the region was 0.1, so the change in absolute intensity was more than ten times the size of the noise in the region. Furthermore, the echo intensity changes were correlated to mechanical changes in the tendon, but the ability of the ultrasound data to predict stress values was not rigorously examined; this could be a potentially interesting avenue to pursue with future work.

Although mechanisms need further elucidation, we have shown that time-dependent mechanical properties during viscoelastic testing are manifested in ultrasonic echo intensity changes. Though the patterns of the echo intensity changes do not directly mimic the patterns of viscoelastic load changes (increasing where load would decrease), the intensity changed in a repeatable (and therefore predictable) fashion. Thus, the viscoelastic echo intensity behavior can be anticipated during future testing. This phenomenon could potentially lead to a more extensive characterization of *in vivo* tissue behavior.

Acknowledgment

Support by the National Science Foundation (award 0553016) and National Institutes of Health (award R21 EB 008548) is gratefully acknowledged.

References

- [1] Ker, R. F., Bennett, M. B., Bibby, S. R., Kester, R. C., and Alexander, R. M., 1987, "The Spring in the Arch of the Human Foot," *Nature*, **325**(6100), pp. 147–149.
- [2] Hingorani, R. V., Provenzano, P. P., Lakes, R. S., Escarcega, A., and Vanderby, R., Jr., 2004, "Nonlinear Viscoelasticity in Rabbit Medial Collateral Ligament," *Ann. Biomed. Eng.*, **32**(2), pp. 306–312.
- [3] Provenzano, P., Lakes, R., Keenan, T., and Vanderby, R., Jr., 2001, "Nonlinear Ligament Viscoelasticity," *Ann. Biomed. Eng.*, **29**(10), pp. 908–914.
- [4] Rumian, A. P., Wallace, A. L., and Birch, H. L., 2007, "Tendons and Ligaments Are Anatomically Distinct But Overlap in Molecular and Morphological Features—A Comparative Study in an Ovine Model," *J. Orthop. Res.*, **25**(4), pp. 458–464.
- [5] Woo, S. L., Gomez, M. A., and Akeson, W. H., 1981, "The Time and History-Dependent Viscoelastic Properties of the Canine Medial Collateral Ligament," *J. Biomech. Eng.*, **103**(4), pp. 293–298.
- [6] Bonifasi-Lista, C., Lakez, S. P., Small, M. S., and Weiss, J. A., 2005, "Viscoelastic Properties of the Human Medial Collateral Ligament Under Longitudinal, Transverse and Shear Loading," *J. Orthop. Res.*, **23**(1), pp. 67–76.
- [7] Dommelen, J. A. W., Jolandan, M. M., Ivarsson, B. J., Millington, S. A., Raut, M., Kerrigan, J. R., Crandall, J. R., and Diduch, D. R., 2006, "Nonlinear Viscoelastic Behavior of Human Knee Ligaments Subjected to Complex Loading Histories," *Ann. Biomed. Eng.*, **34**(6), pp. 1008–1018.
- [8] Heimdal, A., Støylen, A., Torp, H., and Skjærpe, T., 1998, "Real-Time Strain Rate Imaging of the Left Ventricle by Ultrasound," *J. Am. Soc. Echocardiogr.*, **11**(11), pp. 1013–1019.
- [9] D'hooge, J., Heimdal, A., Jamal, F., Kukulski, T., Bijnens, B., Rademakers, F., Hatle, L., Suetens, P., and Sutherland, G. R., 2000, "Regional Strain and Strain Rate Measurements by Cardiac Ultrasound: Principles, Implementation and Limitations," *Eur. J. Echocardiogr.*, **1**(3), pp. 154–170.
- [10] Ophir, J., Céspedes, I., Ponnekanti, H., Yazdi, Y., and Li, X., 1991, "Elastography: A Quantitative Method for Imaging the Elasticity of Biological Tissues," *Ultrason. Imaging*, **13**(2), pp. 111–134.
- [11] Ophir, J., Céspedes, I., Garra, B., Ponnekanti, H., Huang, Y., and Maklad, N., 1996, "Elastography: Ultrasonic Imaging of Tissue Strain and Elastic Modulus *In Vivo*," *Eur. J. Ultrasound*, **3**(1), pp. 49–70.
- [12] Itoh, A., Ueno, E., Tohno, E., Kamma, H., Takahashi, H., Shiina, T., Yamakawa, M., and Matsumura, T., 2006, "Breast Disease: Clinical Application of US Elastography for Diagnosis," *Radiology*, **239**(2), pp. 341–350.

- [13] Crevier-Denoix, N., Ravary-Plumioën, B., Evrard, D., and Pourcelot, P., 2009, "Reproducibility of a Non-Invasive Ultrasonic Technique of Tendon Force Measurement, Determined *In Vitro* in Equine Superficial Digital Flexor Tendons," *J. Biomech.*, **42**(13), pp. 2210–2213.
- [14] Arda, K., Ciledag, N., Aktas, E., Aribas, B. K., and Köse, K., 2011, "Quantitative Assessment of Normal Soft-Tissue Elasticity Using Shear-Wave Ultrasound Elastography," *Am. J. Roentgenol.*, **197**(3), pp. 532–536.
- [15] Catheline, S., Gennisson, J.-L., and Fink, M., 2003, "Measurement of Elastic Nonlinearity of Soft Solid With Transient Elastography," *J. Acoust. Soc. Am.*, **114**(6), p. 3087–3091.
- [16] Evans, A., Whelehan, P., Thomson, K., McLean, D., Brauer, K., Purdie, C., Jordan, L., Baker, L., and Thompson, A., 2010, "Quantitative Shear Wave Ultrasound Elastography: Initial Experience in Solid Breast Masses," *Breast Cancer Res.*, **12**(6), p. R104.
- [17] Sebag, F., Vaillant-Lombard, J., Berbis, J., Griset, V., Henry, J. F., Petit, P., and Oliver, C., 2010, "Shear Wave Elastography: A New Ultrasound Imaging Mode for the Differential Diagnosis of Benign and Malignant Thyroid Nodules," *J. Clin. Endocrinol. Metabolism*, **95**(12), pp. 5281–5288.
- [18] Hughes, D., and Kelly, J., 1953, "Second-Order Elastic Deformation of Solids," *Phys. Rev.*, **92**(5), pp. 1145–1149.
- [19] Kobayashi, H., and Vanderby, R., 2005, "New Strain Energy Function for Acoustoelastic Analysis of Dilatational Waves in Nearly Incompressible, Hyper-Elastic Materials," *J. Appl. Mech.*, **72**(6), pp. 843–851.
- [20] Kobayashi, H., and Vanderby, R., 2007, "Acoustoelastic Analysis of Reflected Waves in Nearly Incompressible, Hyper-Elastic Materials: Forward and Inverse Problems," *J. Acoust. Soc. Am.*, **121**(2), pp. 879–887.
- [21] Duenwald, S., Kobayashi, H., Frisch, K., Lakes, R., and Vanderby, Jr., R., 2011, "Ultrasound Echo is Related to Stress and Strain in Tendon," *J. Biomech.*, **44**(3), pp. 424–429.
- [22] Pan, L., Zan, L., and Foster, F. S., 1998, "Ultrasonic and Viscoelastic Properties of Skin Under Transverse Mechanical Stress *In Vitro*," *Ultrasound Medicine Biol.*, **24**(7), pp. 995–1007.
- [23] Duenwald, S. E., Vanderby, R., and Lakes, R. S., 2010, "Stress Relaxation and Recovery in Tendon and Ligament: Experiment and Modeling," *Biorheology*, **47**(1), pp. 1–14.
- [24] Duenwald, S. E., Vanderby, R., and Lakes, R. S., 2009, "Viscoelastic Relaxation and Recovery of Tendon," *Ann. Biomed. Eng.*, **37**(6), pp. 1131–1140.
- [25] Abrahams, M., 1967, "Mechanical Behaviour of Tendon *In Vitro*," *Med. Biol. Eng.*, **5**(5), pp. 433–443.
- [26] Rigby, B. J., Hirai, N., Spikes, J. D., and Eyring, H., 1959, "The Mechanical Properties of Rat Tail Tendon," *J. Gen. Physiol.*, **43**(2), pp. 265–283.
- [27] Han, S., Gemmell, S. J., Helmer, K. G., Grigg, P., Wellen, J. W., Hoffman, A. H., and Sotak, C. H., 2000, "Changes in ADC Caused by Tensile Loading of Rabbit Achilles Tendon: Evidence for Water Transport," *J. Magn. Reson.*, **144**(2), pp. 217–227.
- [28] Hannafin, J. A., and Arnoczky, S. P., 1994, "Effect of Cyclic and Static Tensile Loading on Water Content and Solute Diffusion in Canine Flexor Tendons: An *In Vitro* Study," *J. Orthop. Res.*, **12**(3), pp. 350–356.
- [29] Helmer, K. G., Wellen, J., Grigg, P., and Sotak, C. H., 2004, "Measurement of the Spatial Redistribution of Water in Rabbit Achilles Tendon in Response to Static Tensile Loading," *J. Biomech. Eng.*, **126**(5), pp. 651–656.
- [30] Itoh, A., Ueno, E., Tohno, E., Kamma, H., Takahashi, H., Shiina, T., Yamakawa, M., and Matsumura, T., 2006, "Breast Disease: Clinical Application of US Elastography for Diagnosis," *Radiology*, **239**, pp. 341–350.
- [31] Zhi, H., Ou, B., Luo, B. M., Feng, X., Wen, Y. L., and Yang, H. Y., 2007, "Comparison of Ultrasound Elastography Mammography and Sonography in the Diagnosis of Solid Breast Lesions," *J. Ultrasound Med.*, **26**(6), pp. 807–815. Available at <http://www.jultrasoundmed.org/content/26/6/807.short>